Effect of speciation transformation on the coagulation behavior of Al_{13} and Al_{13} aggregates

Xiaohong Wu, Changqing Ye, Dongsheng Wang, Xiaopeng Ge and Hongxiao Tang

ABSTRACT

Flocculation of kaolin suspension with aluminium fractal polycations was investigated as a function of aluminium concentration and pH. Aluminium flocculants included Al_{13} and Al_{13} aggregates with OH/Al ratio of 2.6 and 2.8, respectively. The flocculation kinetics and floc size distribution were monitored by light scattering. The characterization of flocculants showed that the tridecatmer Al_{13} and bridged $[Al_{13}]_n$ with out-sphere structure were the dominant species for all flocculants in a wide pH range. The coagulation results indicated that the pre and *in situ*-formed $[Al_{13}]_n$ play a key role in removing particles. With the increasing concentration of $[Al_{13}]_n$, coagulation mechanisms were transformed from charge-neutralization, electro-patch coagulation to bridge-aggregation. Moreover, sweep-flocculation was involved at higher dosage besides other three mechanisms when amorphous aluminium oxides formed. Hence, chemical interaction between particles and flocculants evolved from surface adsorption to surface precipitation for aluminium polycations by virtue of species transformation.

Key words | adsorption, Al_{13}, Al_{13} aggregates, coagulation

Xiaohong Wu
Dongsheng Wang
Xiaopeng Ge
Hongxiao Tang
State Key Lab of Environmental Aquatic Chemistry,
RCEES, Chinese Academy of Sciences,
POB 2871, Beijing 100085,
China
E-mail: *wu_sherry@126.com*;
wgds@rcees.ac.cn;
xpge@rcees.ac.cn;
tanghx@rcees.ac.cn

Changqing Ye
Yantai Institute of Coastal Zone Research for Sustainable Development,
RCEES, Chinese Academy of Sciences,
Yantan
China
E-mail: *eastcqyz@163.com*

INTRODUCTION

Inorganic Polymer Flocculants (IPFs) have gained an increased usage in water treatment industry due to cost reduction and efficiency in particle and organic removal (Edzwald 1993; Duan & Gregory 2003; Sinha *et al.* 2004; Tang & Wang 2004). As one of the most efficient IPFs, poly-aluminium chloride (PACl) got much attention owing to its high content of $Al_{13}(O)_4(OH)_{24}^{7+}$, for which many studies have demonstrated its efficiency on the PACl coagulation process (Gray *et al.* 1995; Tang & Wang 2004; Kazpard *et al.* 2006). Since it was identified and confirmed, the nano-sized tridecameric Al polyoxocation, known as Al_{13}, has drawn much attention on its formation and transformation under various conditions, i.e. the pH, aluminium concentration and organic ions (Bottero *et al.* 1987; Furrer *et al.* 1992, 1999; Molis *et al.* 1996; Amirbahman *et al.* 2000; Casey *et al.* 2000). Generally, the Al_{13} remains stable at the optimal pH (~5) and relative low concentration ($<10^{-3}$ M) in the absence of organic substances and minerals. However, it was found that positive charge of Al_{13} maintains when pH below 6 (Furrer *et al.* 1992), and aggregates and precipitates appears when pH > 6 (Furrer *et al.* 1999). Also, chemical and structural transformation of Al_{13} could be promoted by salicylate ligand (Molis *et al.* 1996). According to current water treatment practices and priorities, the removal of natural organic matter (NOM) by coagulation has assumed greater importance and polyaluminium has outperformed conventional coagulation in many circumstances. In this regard, the transformation of Al_{13} during coagulation would strongly influence the effectiveness, whereas few papers are available and mechanisms are not yet clear.

Investigation suggested that the Al_{13} transformed from the gel with open fractal structure to the bayerite hydroxide

doi: 10.2166/wst.2009.064

upon base hydrolysis and aging, and a major rearrangement of of Al_{13} must take place when hydrolysis advanced to OH/Al ratio of 3.0 (Bottero *et al.* 1987; Bradley *et al.* 1993; Ye *et al.* 2007*a*,*b*). As various aluminium species interact with particles through different pathways, dominant coagulation mechanisms were initiated and faded away during the coagulation process with varied Al concentration, pH and other conditions. What happens to the Al_{13} from independent particles to bridged aggregates and finally amorphous oxides means a lot to the coagulation behavior of polyaluminium with pre-formed Al_{13}, and yet few studies have been investigated on.

The goal of this study is to investigate the effect of Al_{13} transformation on coagulation. The coagulation behaviors of Al_{13} and Al_{13} aggregates with kaolin suspension were studied as a function of Al concentration and pH. Al_{13} transformation was examined by ferron assay under various pH. The particle aggregation was also monitored by light scattering, trying to interpret coagulation mechanisms through flocculation kinetics and jar test results.

MATERIALS AND METHODS

Kaolin suspension

Kaolin suspension was made by kaolin clay with deionized water. A stock suspension of kaolin clay was prepared by dispersing a measured amount of reagent-grade kaolin in deionised water by high shear mixing. The stocked solid content was determined gravimetrically and found to be 74 g/l. Particle size distribution and zeta potential of the kaolin suspension was measured by Mastersizer 2000 (Malvern Co., UK) and Zetasizer 2000 (Malvern Co., UK), respectively. The mean particle size of suspension was 2.2 μm. The working suspension was prepared by diluting a calculated amount of stock suspension with half tap water and half deionzed water.

Coagulants

Preparation and speciation

The preparation of tridecamer Al_{13} and Al_{13} aggregates with B (OH/Al) values of 2.6 and 2.8 was same as what reported in our previous study, and the characterization of Al species used the same procedure of Ferron assay and ^{27}Al NMR (Wu *et al.* in press). The operation parameters of NMR were NS = 128, P1 = 20 μs, PL1 = −3 dB, $T = 298$ K. Speciation of all the coagulants by Ferron assay were determined every day and found that remains stable in a month after one-week-aging. The coagulation tests were performed using weekly-aged coagulants in this regard, and the speciation of weekly-aged coagulants is summarized in Table 1.

To characterize the speciation transformation during coagulation process, the diluted solutions of Al_{13} and aggregates were examined at the total aluminium concentration of 10^{-4} mol/L under the same condition as jar test without particles. Accordingly, ferron assay procedure included two steps: one is 2 minutes after coagulant injection and the other after 30 minutes.

Coagulation test

Jar test was performed by a JTY laboratory stirrer (Daiyuan Company, Beijing) in a 500 ml working suspension following procedure as: 2 min rapid mixing (200 rpm), 10 min slow mixing (40 rpm) and 15 min sedimentation. The zeta potential and residual turbidity were measured separately after rapid mixing and sedimentation, with Malvern Zetasizer 2000 and HACH 2100N turbidity meter, respectively. Suspension's pH was adjusted prior to the coagulant injection with HCl (0.05 M) or NaOH (0.05 M) and was not readjusted after coagulant injection as pH drop resulting from hydrolysis can be neglected. Particle size distribution was determined by small-angle static light scattering with Malvern Mastersizer 2000. The instrument determined the scattered intensity at measuring angles ranging from 0°–46° with a He-Ne laser light of 632.8 nm. An integration time of 40 s per curve was chosen to compromise measuring speed and data quality. The size information of aggregated

Table 1 | The Al species distribution of coagulants

Coagulants	Al_T (mol/L)	Ferron assay (%) Al_a	Al_b	Al_c	^{27}Al NMR (%) Al_{13}	pH
B2.46	0.05	5.0	95.0	0	99	5.26
B2.6	0.05	3.4	71.5	25.1	67	5.80
B2.8	0.05	2.9	61.6	35.4	0	5.98

particles was monitored during coagulation using standard 1L glass beaker connecting with the instrument to perform the same procedure as jar test.

RESULTS AND DISCUSSION

Coagulants species transformation

Although large amount of studies have been addressed on the chemical speciation of hydrolyzed aluminium, disagreement on the species transformation has been existed since it was first reported (Bertsch & Parker 1996; Bi *et al.* 2004). From the results shown in Table 1, it is evident that species transformation varies with the increasing B values. For the B2.46 (structural OH/Al ratio of Al_{13}) solution, tridecamer dominates the species distribution while the other three exhibits not only tridecamer but also sol-gels leading to the unclear solution for B2.8 solution. Comparing the species analysis measured by ferron assay and ^{27}Al NMR, it can be seen that Al_b almost equals to Al_{13} for B2.46, 2.6, while Al_{13} decrease fast and disappeared for B2.8 when Al_b still remains relatively high. As a result, structure rearrangement can be suggested to occur during further alkalinification, while the active prosperity of Al_{13} was maintained to contact with ferron colorimetric solution. As tridecamer Al_{13} is prone to form larger polymer or colloidal Al species with increasing B values, re-dissolving of the precipitates will not lead to the formation of Al_{13} for the aggregated Al_{13} of high B values approaching to 3.0 (Ye *et al.* 2007*a*). However, decomposition of Al_{13} and Al_{13} aggregates happens at lower B values. As Figure 1 indicates that the Al_b portions decrease in the acidic range for B2.46 and B2.6, although they maintain relatively stable in the whole pH range. For B2.8, a slow decrease of Al_b can be observed from acidic to alkaline side. Obviously, this part of Al_b transformed to Al_c swiftly *in situ* due to hydroxyl complexation. On the other hand, the Al_b portions reduce ~40% and 20% for B2.46 and B2.6 at pH6.3 after 30 mins reaction. This may be attributed to the fast decomposition rate of Al_{13} (Furrer *et al.* 1999), yet investigation needs to be paid on this issue further. If we assigned $[Al_{13}]_n$ to the aggregated Al_{13}, the polymeric scale can be explained by the value of n. Species

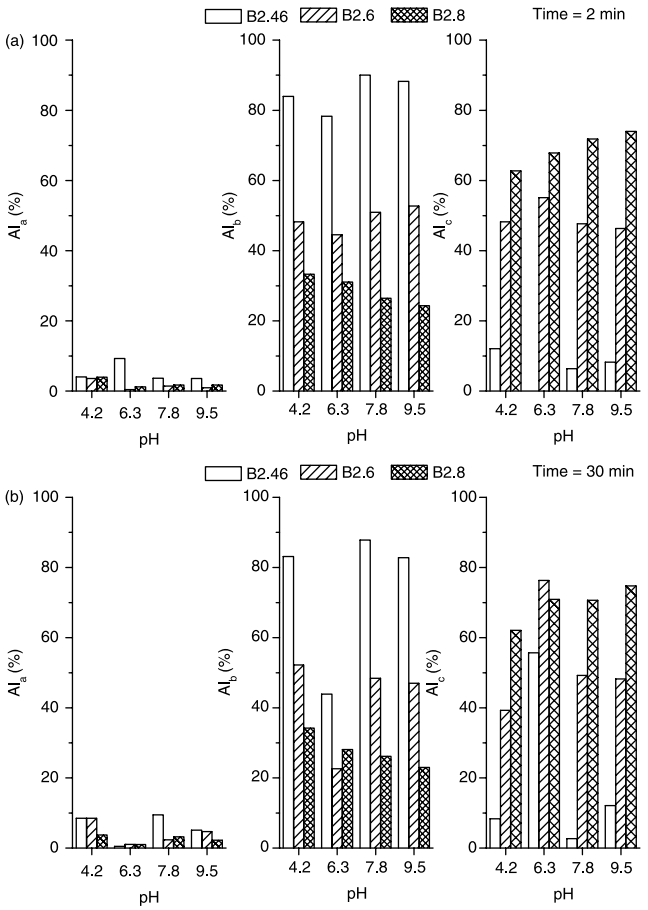

Figure 1 | Species distribution of coagulants varies with pH values reacting after 2 minutes and 30 minutes. The total aluminium concentration is 10^{-4} mol/L.

transformation of Al_{13} relate to n and structure rearrangement may occur with excess n. However, the quantification of n has not been well studied though some researchers published the numbers of Al_{13} for B2.46 and B2.6 (Lartiges *et al.* 1997).

Coagulation results

Particle removal and ζ-potential

Jar test were performed using 50 mg/L working suspension. The initial turbidity, zeta potential and pH were 70 ± 2 NTU, -19.5 ± 0.5 mv and 7.5 ± 0.2, respectively. The effect of coagulant dosage as aluminium concentration on the zeta potential and turbidity removal is shown in Figure 2(a) and (b). It can be seen that the zeta potential increased rapidly and reversed quickly with low dosage for

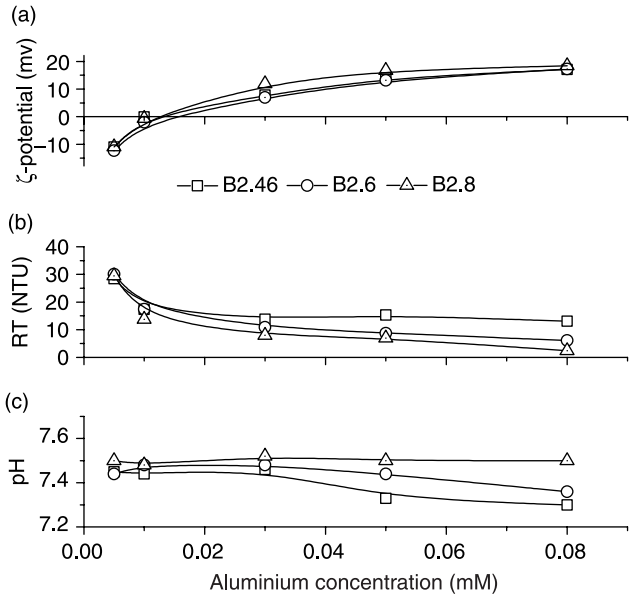

Figure 2 | Coagulation evolution as a function of aluminium concentration of (a) ζ-potential, (b) residual turbidity, (c) pH values. Kaolin suspension: 50 mg/L, pH: 7.5.

all the flocculants. The CCC (Critical Coagulation Concentration) of all the flocculants were low at 0.01 mM and a higher turbidity removal can be observed reaching 75%. With increasing dosage, residual turbidity for suspensions adding Al_{13} aggregates decreased and down to the lowest about 2 NTU, while a turbidity value of 10 NTU was observed for suspensions injected with pure Al_{13}. Although the charge reversal happened at the low dosage for all flocculants, the re-stabilization doesn't occur for each. Obviously, different coagulation mechanisms were involved resulting from the species transformation *in situ* and preformed alkalification. As the tridecamer Al_{13} transformed into larger polymer or colloidal cluster with increased B values, more Al_{13} units can be dissociated from the aggregated Al_{13} upon rapid stirring for the lower B-value aggregates (B2.46, B2.6), whereas less Al_{13} units were released for B2.7 and B2.8. Previous study indicated that charge-neutralization, electro-patch coagulation and bridge-aggregation were included for the coagulation mechanism of PACl with high content Al_{13} (Wu *et al.* 2007). At low dosage of 0.005 mM, turbidity removals were ~50% for all the flocculants while zeta potentials remained negative at ~ − 10 mv. This kind of coagulation behavior can be attributed to the positive "electrostatic-patches" over portions of particle surface which enhance the particle aggregation by adsorbing negatively charged particle surface (Ye *et al.* 2007*b*). For their most species were stable positively Al_b polymer (>60%), all the flocculants manifested strong charge-neutralization and electrostatic-patch coagulation mechanisms resulting form the rapid adsorption of species onto the particle surfaces at the lower dosage (Wu *et al.* 2007).

Particle aggregation

The aggregation of particles is greatly influenced by various inter-particle forces such as electrostatic repulsion since most of them are negatively charged. Destablized particles collide with each other with consequent suspension agitation. The final size of aggregated particles or floc is related to collision efficiency, initial particle size distribution and particle concentration etc. As Figure 3 shows, particle aggregation induced by different flocculants is quite distinct owing to their species distribution and transformation. For the lower dosage of 0.01 mM, pure Al_{13} exhibited the fastest size increasing rate with final floc size reached to 108.8 μm after slow mixing, although the largest floc size of 110.6 μm is observed for B2.8. At higher dosage of 0.08 mM, floc size evolution depended much on the B values as Figure 3(b) indicates. After rapid mixing, fine particles with size less than 1 μm (Figure 3(a) shows) disappeared and flocs size enlarged from 50.4 μm to 332.1 μm with increasing B values. The largest floc size observed (603.2 μm) is also related to the highest B value under this condition. Therefore, aggregated Al_{13} outperformed pure Al_{13} in particle aggregation and agglomeration due to their species characteristics. It was reported that Keggin Al_{13} ($d \sim 2$ nm) can be bridged into $[Al_{13}]_n$ via anions and maintain Al_{13} structure under certain neutralization (Bertsch & Parker 1996). According to the speciation results in Table 1 and Figure 1, it can be suggested that at least a portion of bridging $[Al_{13}]_n$ are included in the aggregated Al_{13} besides amorphous hydroxide or sol-gel. This kind of $[Al_{13}]_n$ catalyzed particle aggregation in terms of improving effective collisions (larger size flocculants) and rapid adsorption (higher positive charge compared with hydroxide precipitates). As a result, faster aggregation occurred and large floc formed instantly for the Al_{13} aggregates. In this regard, bridging-aggregation performed shortly after injection for all the flocculants. With further

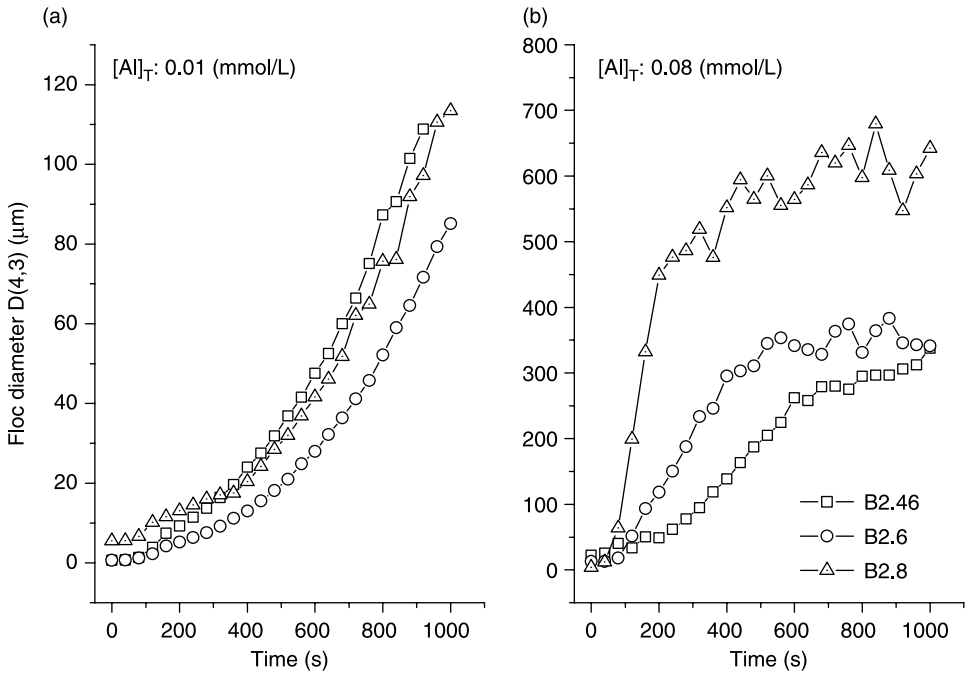

Figure 3 | Flocs diameter of D (4,3) versus coagulation time at two constant dosage (raw water pH 7.5, raw water turbidity 70 NTU).

stirring, flocculants with high B values were prone to precipitate on the particle surfaces or in the solution due to hydroxyl compensation.

pH effect on the coagulation behaviors

Figure 4 shows the pH effect on the zeta potential and particle removal at two constant dosages of 0.01 and 0.08 mM Al/L with pH range of 4 ~ 10. At lower aluminium dosage, Al_{13} exhibited lower particle removal at the acidic range pH < 6 while improved greatly when pH > 6 and then levels off around 20 NTU. It can be inferred that portions of $[Al_{13}]_n$ was decomposed by protons in acidic solution and formation of $[Al_{13}]_n$ was inhibited on the contrary. With more $[Al_{13}]_n$ formed during alkalification, aggregated Al_{13} can well resist the pH shock and outperformed pure Al_{13} in the acidic range (Figure 1). With the increasing pH, hydroxide precipitates appeared upon further neutralization for high B-valued flocculants and more $[Al_{13}]_n$ formed for B2.46. Hence the charge-neutralization, electro-patch coagulation and also bridge-aggregation induced by $[Al_{13}]_n$ were weaker along with the increased B values. This can also be observed at the higher dosage except sweep-flocculation was boosted for high B-valued flocculants in the presence of active amorphous precipitates within the alkali range. The residual turbidity reversed with B values at pH ~ 10 since much more hydroxyl promoted the formation of solid precipitates with less activity.

DISCUSSION

Destabilization and adsorption

Destabilization of negative colloidal particles in natural water can be achieved alone DLVO lines by decreasing diffuse thickness using salts or specific adsorption of highly charged cationic to neutralize particles. Also polymer additives can cause particle aggregation by bridging or charge-neutralization (Duan & Gregory 2003). From the speciation distribution in the various pH values in Figure 1, the predominant species of all the coagulants are poly-nuclear hydrolysis products during coagulation process. However, different polymeric products are assigned to each coagulant as Al_b for B2.46 (Al_{13}) and $Al_b + Al_c$ for B2.6 and Alc for B2.7, B2.8. Therefore, destabilization can be distinct

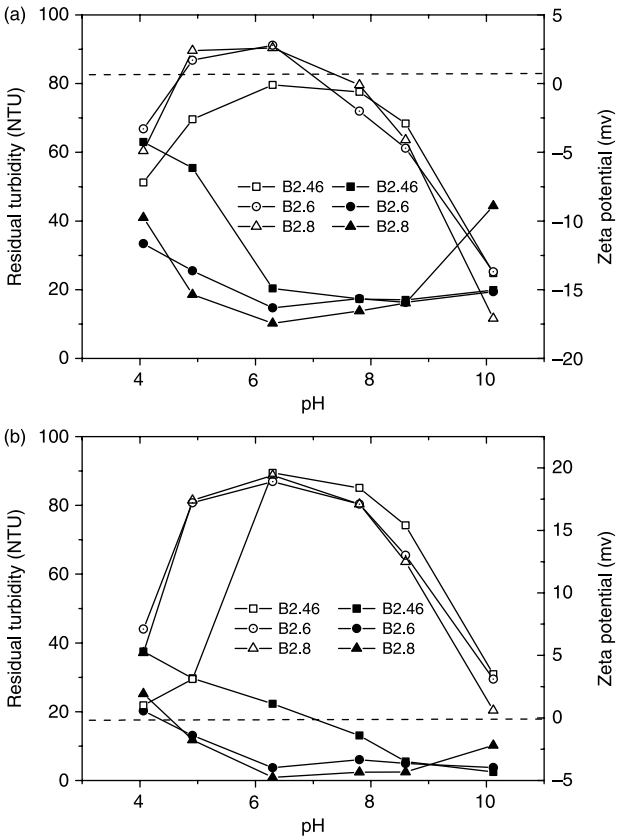

Figure 4 | Effect of pH to the particle removing ζ-potential at two constant aluminium concentrations: a: 0.01 mmol/L; b: 0.08 mmol/L (open: zeta potential, filled: residual turbidity).

from Al_{13} to Al_{13} aggregates since their charges and structures may be distinct according to the previous reports (Bottero *et al.* 1990; Casey *et al.* 2000; Duan & Gregory 2003). The pH independence of Al_{13} molecular decomposition in acidic ph was shown indirectly in Figure 1 by Ferron assay speciation and it agreed well with previous study (Casey *et al.* 2000). Compared with aggregated Al_{13}, particle destabilization of Al_{13} is caused mostly by highly positive Al_{13}^{7+} strongly adsorbing on the negative particles at both lower and higher aluminium dosage. Owing to the monolayer adsorption model of Al_{13}, particles covered with positive polycations turn to reversal charges and begin to repel each other at very low aluminium concentration ($\sim$0.01 mmol/L, shown in Figure 2 and Figure 4). While for Al_{13} aggregates, the active adsorbent include not only highly positive polycations but also sol-gel polymeric hydrolysis products or even amorphous hydroxide. They exhibited stronger charge-neutralization ability in acidic pH since decomposed aggregated Al_{13} may introduce Al_{13} unit and lead to an enhanced adsorption. As Figure 2(a) and (b) indicate that CCC of aggregated Al_{13} were about 0.01 mmol/L which means particle destabilization occurred at that time. Again we notice the unusual behaviors of B2.46 and B2.6 under pH 6. From the speciation transformation in Figure 1, some media polymeric species transferred to larger ones at pH 6 for coagulants B2.46 and B2.6 during the coagulation process.

Chemical interaction evolution

Previous studies indicated pre-hydrolyzed coagulants are often found to be more effective than traditional coagulants owing to their substantial component of tridecamer Al_{13} (Gray *et al.* 1995; Tang & Wang 2004; Kazpard *et al.* 2006). Although controversy still exists for the formation process of tridecamer Al_{13}, most reports agree that Al_{13} is stable and can be readily available for adsorption and charge-neutralization. From the speciation distribution of initial coagulants and their hydrolysis products in different pH at this study, chemical interactions between particles and coagulants varied resulting from distinctive speciation. With high proportion of Al_b, pure Al_{13} displayed its strong adsorption ability due to the highly positive $Al_{13}O_4(OH)_{24}^{7+}$ and formed relatively small and compact flocs. For the further neutralized Al_{13} aggregates, coagulation behaviors developed with the increasing B values. Considering the equal proportion of Al_b and Al_c for B2.6, not only the high positive Al_{13} but also positive sol-gel or amorphous hydroxides contact with negative particles by adsorption. Furthermore, sweep flocculation occurred owing to the precipitation deposited on the particle surface and in the solution. With adding base, positive precipitation contributed much to the formation of larger and loose flocs for B2.7 and B2.8. Although precipitation are involved in the coagulation process of aggregated Al_{13}, it is not the same as traditional "alum" which former study had demonstrated the quite different nature of their precipitations (Van Benschoten *et al.* 1990). The zeta potential of aggregates are higher than pure Al_{13} in the pH range 4 $\sim$ 7, which means that the aggregates decomposed in the solution and formed polyocations or Al_{13} again. The larger aggregated polymer during further alkalinification may result from Al_{13}

assembling which is active to the ferron agent but can't be detect by the NMR. Although the surface precipitation of Al_{13} may appear in the pH above 6, the newly formed Al_{13} is also subjected to the acid-catalyzed decomposition and reformation (Furrer *et al.* 1999). Some reports proved that the decomposition reaction can be described as the function of free proton concentration and the half-life at pH 5 reached to hundreds hours (Furrer *et al.* 1999). Therefore, it can be inferred that the Al_{13} aggregates are combined by the hydroxyl forming larger particles and decomposed when OH group reacted with free protons in the solution. Because of less hydroxyl groups, the pure Al_{13} decompose more easily to form minor polynuclear species, while the aggregates turned to the Al_{13} first and thus improve the positive charge in the acidic range. With extra binding hydroxyl, the Al_{13} aggregates could create much more amorphous Al $(OH)_3$ than pure Al_{13} does in the same period. Furthermore, aggregates adsorbed on the surface of colloidal particles may form a high positive electronic-patch which may attract on the negative colloidal particles and thus the patch-coagulation also account for the rapid rise of flocs size (Ye *et al.* 2007*b*). The pH depression of Al_{13} aggregates are less than pure Al_{13}, while the turbidity removal remains high above pure Al_{13} especially for the aggregate with higher basicity and larger particle size. The benefits of Al_{13} aggregates can enhance the charge neutralization ability of pure Al_{13} and make up its shortage of amorphous hydroxide.

ACKNOWLEDGEMENTS

The authors would like to thank the National Natural Science Foundation of China (NSFC) in support of this project (No. 20537020, No. 50678167 and No. 20677073).

REFERENCES

Amirbahman, A., Gfeller, M. & Furrer, G. 2000 Kinetics and mechanism of ligand-promoted decomposition of the Keggin Al-13 polymer. *Geochim. Cosmochim. Acta* **64**(5), 911–919.

Bottero, J. Y., Axelos, M., Tchoubar, D., Cases, J. M., Pripiat, J. J. & Fiessinger, F. 1987 Mechanism of formation of aluminium trihydroxide from Keggin Al_{13} polymer. *J. Colloid Interface Sci.* **117**(1), 47–57.

Bottero, J. Y., Tchoubar, D., Axelos, M. A. V., Quienne, P. & Fiessinger, F. 1990 Flocculation of silica colloids with hydroxy aluminium polycations. Relation between floc structure and aggregation mechanisms. *Langmuir* **6**(3), 596–602.

Bradley, S. M., Kydd, R. A. & Howe, R. F. 1993 The structure of Al gels formed through the base hydrolysis of Al^{3+} aqueous solutions. *J. Colloid Interface Sci.* **159**(2), 405–412.

Bertsch, P. M. & Parker, D. R. 1996 Aqueous polynuclear aluminium species. *The Environmental Chemistry of Aluminium*. CRC Press, Boca Raton, FL, pp. 117–168.

Bi, S. P., Wang, C. Y., Cao, Q. & Zhang, C. 2004 Studies on the mechanism of hydrolysis and polymerization of aluminium salts in aqueous solution: correlations between the "Core-links" model and "Cage-like" Keggin-Al_{13} model. *Coord. Chem. Rev.* **248**(5-6), 441–455.

Casey, W. H., Phillips, B. L., Karlsson, M., Nordin, S., Nordin, J. P., Sullivan, D. J. & Neugebauer-Crawford, S. 2000 Rates and mechanisms of oxygen exchanges between sites in the $AlO_4Al_{12}(OH)_{24}(H_2O)_{12}^{7+}$(aq) complex and water: implications for mineral surface chemistry. *Geochim. Cosmochim. Acta* **64**(17), 2951–2964.

Duan, J. & Gregory, J. 2003 Coagulation by hydrolysing metal salts. *Adv. Colloid Interface Sci.* **100–102**, 475–502.

Edzwald, J. K. 1993 Coagulation in drinking water treatment: particles, organics and coagulants. *Water Sci. Technol.* **27**(11), 21–35.

Furrer, G., Ludwig, C. & Schindler, P. W. 1992 On the chemistry of the Keggin Al_{13} polymer: I. Acid-base properties. *J. Colloid Interface Sci.* **149**(11), 56–67.

Furrer, G., Gfeller, M. & Wehrli, B. 1999 On the chemistry of the Keggin Al-13 polymer: kinetics of proton-promoted decomposition. *Geochim. Cosmochim. Acta* **63**(19-20), 3069–3076.

Gray, K. A., Yao, C. H. & O'Melia, C. R. 1995 Inorganic metal polymers: preparation and characterization. *J. Am. Water Works Assoc.* **87**(4), 136–146.

Kazpard, V., Lartiges, B. S., Frochot, C., de la Caillerie, J. B. D., Viriot, M. L., Portal, J. M., Gorner, T. & Bersillon, J. L. 2006 Fate of coagulant species and conformational effects during the aggregation of a model of a humic substance with Al-13 polycations. *Water Res.* **40**(10), 1965–1974.

Lartiges, B. S., Bottero, J. Y., Derrendinger, L. S., Humbert, B., Tekely, P. & Suty, H. 1997 Flocculation of colloidal silica with hydrolyzed aluminium: an ^{27}Al solid state NMR investigation. *Langmuir* **13**(2), 147–152.

Molis, E., Thomas, F., Bottero, J. Y., Barres, O. & Masion, A. 1996 Chemical and structural transformation of aggregated Al_{13} polycations, promoted by salicylate ligand. *Langmuir* **12**(13), 3195–3200.

Sinha, S., Yoon, Y., Amy, G. & Yoon, J. 2004 Determining the effectiveness of conventional and alternative coagulants through effective characterization schemes. *Chemosphere* **57**(9), 1115–1122.

Tang, H. X. & Wang, D. S. 2004 Optimization of the concepts for poly-aluminium species. In: Hahn, H. H. & Odegaard, H. (eds) *Chemical Water and Wastewater Treatment*. IWA, London, pp. 139–149.

Van Benschoten, J. E. & Edzwald, J. K. 1990 Chemical aspects of coagulation using aluminium salts–I. Hydrolytic reactions of alum and polyaluminium chloride. *Water Res.* **24**(12), 1519–1526.

Wu, X. H., Ge, X. P., Wang, D. S. & Tang, H. X. 2007 Distinct coagulation mechanism and model between alum and high Al_{13}-PACl. *Colloids Surf. A: Physicochem. Eng. Asp.* **305**(1-3), 89–96.

Wu, X. H., Wang, D. S., Ge, X. P. & Tang, H. X. 2008 Coagulation of silica microspheres with hydrolyzed Al (III)-significance of Al_{13} and Al_{13} aggregates. *Colloids Surf. A Physicochem. Eng. Asp.* **330**, 72–79.

Ye, C. Q., Wang, D. S., Shi, B. Y. & Qu, J. H. 2007*a* Formation and transformation of Al13 from freshly formed precipitate in partially neutralized Al (III) solution. *J. Sol-Gel Sci. Technol.* **41**(3), 257–265.

Ye, C. Q., Wang, D. S., Shi, B. Y., Yu, J. F. & Qu, J. H. 2007*b* Alkalinity effect of coagulation with polyaluminium chlorides: role of electrostatic patch. *Colloids Surf. A: Physicochem. Eng. Asp.* **294**(1–3), 163–173.